

Mechanistic Aspects of Clay Intercalation with Amphiphilic Poly(styrene-*co*-maleic anhydride)-Grafting Polyamine Salts

Jiang-Jen Lin,* Yen-Chi Hsu, and Kuan-Liang Wei

Institute of Polymer Science and Engineering, National Taiwan University, Taipei, Taiwan

Received October 30, 2006; Revised Manuscript Received December 22, 2006

ABSTRACT: The ionic exchange reaction of the smectite clays was affected by using a series of polymeric amine salts, synthesized by grafting poly(oxyalkylene)-diamines (POA-amine) onto poly(styrene-*co*-maleic anhydrides) (SMA). The comb-branched polyamines, comprised of a hydrophobic SMA backbone and multiple amine pendants, are amphiphilic in nature and capable of reducing the toluene/H₂O interfacial tension (from 36 to 4 mN/m at 10⁻³ wt % concentration). After acidification to cationic amines (–NH₃⁺Cl[–]), the polyamines increased solubility in water and effectiveness for the clay intercalation. Depending on the structural variation and their amphiphilic property, the SMA-derived polyamines may intercalate with sodium montmorillonite to yield the organoclays with a broad range of XRD basal spacing from 12.9 to 78.0 Å. The intercalation profile is suspected to proceed with a critical *d* spacing expansion, due to hydrophobic phase separation from the embedded organics in the gallery confinement. The variations of hybrid basal spacing, TGA degradation pattern, and DSC analyses indicated the presence of at least two different types of intercalated hybrids. The finding on clay intercalating mechanism could lead to the synthesis of new organoclays for suiting versatile applications.

Introduction

The naturally occurring layered silicates have a diversity of industrial applications because of their unique characteristics of thin platelet geometric shape, high surface area and intense ionic charge density. Conventionally, the silicate clays have been utilized as catalysts,¹ adsorbents,² metal chelating agents,³ and fillers for polymer composites.⁴ More recently, the clay applications have been extended to the areas of biomaterials such as DNA encapsulations and gene therapy.⁵ For these widespread applications, the clay is commonly required an organic modification. For example, in the applications of polymer/layered silicate nanocomposites, the hydrophilic silicate clays was intercalated with fatty amine surfactants to become compatible with the hydrophobic polymers for improving properties such as gas barrier,⁶ mechanical and thermal stability,⁷ and fire resistance.⁸ Since the first commercial development of the Nylon-6/montmorillonite nanocomposite,⁹ the technology has been extended to other polymers such as polyimide,⁶ polypropylene,¹⁰ polystyrene,¹¹ polyurethane,¹² polyester,¹³ epoxy resins,¹⁴ etc.

The organic modification generally involves the uses of low-molecular-weight alkyl quaternary ammonium salt to exchange with the counterions in the layered silicates. Recently, polymeric types of intercalating agents, such as the copolymer of styrene and vinylbenzyltrimethylammonium chloride,¹⁵ were reported for the improved basal spacing expansion and the compatibility in nanocomposites. Consequently, the embedded organics that are conventionally limited to the surfactant species could be extended to the polyamine salts with hydrophobic polymer backbones. As a result, the organoclays with a high hydrophobic compatibility may be prepared. Recently, we have also reported the use of high-molecular-weight poly(oxyalkylene)-diamine salts (POA-amine, 2000–4000 *M_w*)¹⁶ to modify sodium montmorillonite (Na⁺–MMT). In addition, the amphiphilic polyamines, prepared from the POA-amine grafting

reaction, were found to be effective for intercalation under emulsion conditions.¹⁷ The amphiphilic copolymers possessing polyvalent amine salts as intercalating sites facilitated the intercalation to afford the hybrids at a maximum *d* spacing or practically exfoliation of the Na⁺–MMT layered structure.¹⁸ These results implied that the conventional intercalation process could be performed in an emulsification conditions and the property of organoclays could be tailored. However, the preparation of the copolymers involving the commercially available PP-*g*-MA¹⁹ and SEBS-*g*-MA¹⁷ have a limitation on the low amount of MA functionalities, 4 and 2 wt %, respectively. The amount of the grafting POP-amine may not achieve the desired hydrophilic/hydrophobic balance or multiplicity of the pendent groups. In this report, we synthesized the POA-grafted SMA copolymers as the polyvalent amine salt intercalants, and further evaluated their intercalation mechanism. The structural variation of the SMA backbones allows us to systematically investigate the variants in affecting the *d* spacing, organic embedding fraction, ionic exchanging profile, and also the hydrophobic phase segregation in the confinement.

Experimental Section

Materials. Sodium montmorillonite (Na⁺–MMT; supplied by Nanocor Inc.), is a Na⁺ type of aluminosilicate clay with a cationic exchange capacity (CEC) of 140 mequiv/100 g. The 2:1 type of layered smectite clay is comprised of two tetrahedron sheets sandwiching an edge-shared octahedral sheet, with a polydispersed dimension at average 100 × 100 × 1 nm³ for each sheet, and approximately 8–10 platelets in one stack. Poly(styrene-*co*-maleic anhydride) copolymers with different styrene/maleic anhydride (ST/MA) molar ratios of 1/1, 3/1, 6/1, and 11/1 in the backbones were purchased from Aldrich Chemical Co. or Sino-Japan Chemical Co., with the designated trade names of SMA1000, SMA3000, SMA6000, and SMA11000, respectively. Their averaged molecular weights were estimated to be 6000, 6000, 120 000 and 140 000 *M_w* by GPC, respectively. Poly(oxyalkylene)-diamines (POA-amines) include a family of hydrophobic poly(oxypropylene)-diamines (POP-amines), and hydrophilic poly(oxyethylene)-diamines (POE-amines) of different molecular weights. POE-2000 is a hydrophilic and water-soluble diamine with a POE middle block of 2000 *M_w*.

* Corresponding author. Fax: +886-2-3362-5237. E-mail: jianglin@ntu.edu.tw.

Table 1. Analyses of the SMA–POP Copolymers

SMA–POP copolymer	GPC mol wt	
	M_w	(M_w/M_n)
SMA3000	6000	2.0
POP2000	2900	1.2
SMA3000/POP230	<i>a</i>	<i>a</i>
SMA3000/POP400	<i>a</i>	<i>a</i>
SMA3000/POP2000	13 800	1.2
SMA3000/POP4000	11 800	1.9

^a Insoluble in THF (average molecular weight was estimated by using polystyrene standard).

The POP–amines of 230 and 400 M_w are backbone with low-molecular-weight POP segments and water-soluble, while their high M_w analogs such as 2000 and 4000 M_w are hydrophobic and water insoluble. These POP–amines with 230, 400, 2000, and 4000 M_w , abbreviated as POP230, POP400, POP2000, and POP4000, respectively, were obtained from Aldrich Chemical Co. or Huntsman Chemical Co.

Analytical Instruments. X-ray powder diffractometer (Schimadzu SD-D1 using a Cu target at 35 kV, 30 mA) was used to measure the d spacing of the intercalated silicates. According to the Bragg's equation ($n\lambda = 2d\sin\theta$), the basal spacing of $n = 1$ was calculated on the basis of the observed $n = 2, 3$ and so on. The high basal spacing was confirmed by fine-tuning the wide-angle X-ray diffraction (WAXD) instrument into the range of $2\theta = 1-2^\circ$. The organic fraction in the silicate hybrids was determined by using a thermal gravimetric analyzer (TGA, Perkin-Elmer Pyris 1) at a heating rate of $10^\circ\text{C min}^{-1}$ up to 900°C in air. The interfacial tension was measured by the Wilhelmy method using a Kruss-K10 digital tensiometer equipped with a spherical ring. Gel permeation chromatography (GPC) was performed on Waters apparatus (515 HPLC pump, 717 auto-sample, and 2410 refractive index detector). The Waters Stygel column set was used for analyzing the relative molecular weights under a 1.0 mL/min flow rate of tetrahydrofuran (THF), calibrated against the polystyrene standards. Thermal analyses of melting and crystalline temperatures were carried out by using a differential scanning calorimeter (DSC, Perkin-Elmer Pyris 6). Sample size of 3–8 mg on a sealed aluminum pan was generally used. The temperature range of -20 to $+150^\circ\text{C}$ at a heating rate of $10^\circ\text{C min}^{-1}$ with a nitrogen flow of 20 mL min^{-1} was used. The melting point (T_m) was determined from the thermogram while the enthalpy of crystallization (ΔH) was measured by integrating the peak area.

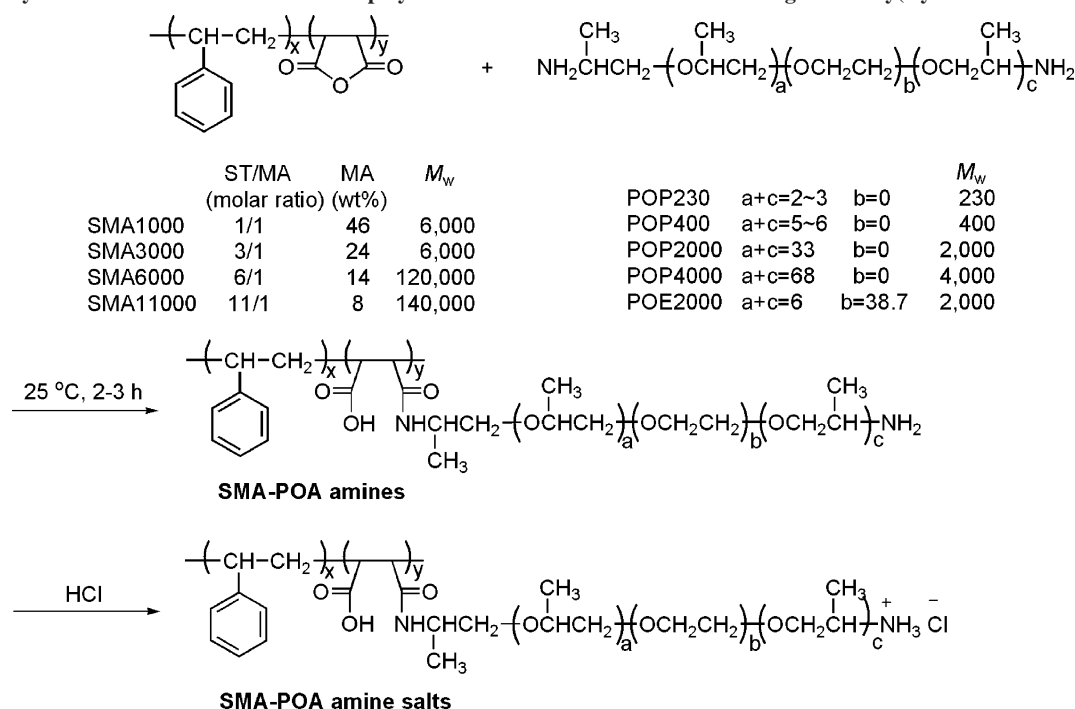
Synthesis of the SMA–POP Copolymers. In the preparative procedures, it is crucial to dry the SMA and POP–amine starting materials at the condition of 120°C in an oven under reduced pressure for 6 h before using. An excess amount of POP–amines in 2-fold equivalents to SMA was employed to avoid the potential cross-linking reaction between the SMA and diamines. An example of preparing POP2000-grafted SMA3000 is described below. To a three-necked and round-bottomed flask, equipped with a mechanical stirrer, was charged POP2000 (97.6 g, 48.8 mmol), followed by the dropwise addition of SMA3000 (10.0 g, 24.4 mmol of MA) in THF (50 mL). Under constant stirring, the mixture was maintained at 25°C for 2–3 h. During the process, samples were taken periodically and monitored by using a FT–IR. The disappearance of the absorption of anhydride functionality at 1780 (s) and 1850 cm^{-1} (w) and the formation of carboxylic acid and amide functionality at 1734 and 1690 cm^{-1} , respectively, was observed. The characteristic absorptions at 1100 cm^{-1} for the oxyalkylene ether were also observed. The reaction products were extracted out the unreacted POP–amines several times by ethanol/water mixture (1:2 by volume). The mixed solvent extraction allowed the removal of excess POP–amines through a separation funnel. The purified product was then analyzed by GPC analysis, as summarized in Table 1. The amine titration showed that the amine weight equivalents of these copolymers to be 560, 500, 2,000, 4000 mequiv/g for SMA3000–POP230, SMA3000–POP400, SMA3000–POP2000, and SMA3000–POP4000, respectively.

Intercalation of Na^+ –MMT with the SMA–POA Copolymers. The typical experimental procedures for the clay interaction are described below. In a 1-L flask equipped with a mechanical stirrer, Na^+ –MMT (0.5 g, 0.7 mequiv) was agitated and swelled in deionized water (50 mL) at 80°C . To a well-dispersed Na^+ –MMT slurry was added SMA3000–POP2000 quaternary ammonium salts (11.8 g, 0.7 mequiv), which were pretreated with HCl (0.11 N, 6.3 mL, 0.7 mmol) in the deionized water at 80°C and stirred for 5–6 h. The resultant precipitates were collected and washed thoroughly with water (for the SMA3000–POP230, –POP400 products) or toluene (for SMA3000–POP2000, –POP4000) to remove the adsorbed SMA–POA polyamines on the clay surface. The product (abbreviated SMA–POA/MMT) was dried in a vacuum oven at 80°C for 24 h before being analyzed by XRD and TGA.

Results and Discussion

Synthesis and Property of the Comb-Branched Amphiphilic Copolymers. A series of comb-branched polyamines were prepared by grafting POA–amine on the SMA, as shown as Scheme 1. The synthesis involves the reaction of cyclic anhydride and amine ($-\text{NH}_2$) to generate an amide in the linking site. The grafting POA–amines include the hydrophobic poly(oxypropylene)– (POP) and hydrophilic poly(oxyethylene)– (POE) backbones with various molecular weights (M_w) ranging from 230 to 4000 g/mol. To avoid the formation of cross-linked polymer, excess equivalents of diamines were allowed to react with the anhydride. After the reaction, the unreacted amines were removed by an additional extraction step with the ethanol/water mixture. FT–IR and amine titration data were analyzed to confirm the product consistency. The synthesis allows the preparation of SMA–POP copolymers with varied styrene/anhydride ratios in the SMA backbone as well as the length and hydrophilic nature of the pendent POA–amines. Hence, the amphiphilic properties and ionic exchanging ability are adjustable when interacting with Na^+ –MMT.

For the ionic exchange reaction with clays, the SMA–POP intercalating copolymers are required to be soluble in water since the ionic clay is hydrophilic and swelled in water. The presence of amide, carboxylic acid, and multiple amine functionalities as the hydrophilic portions and the SMA as the hydrophobic backbone rendered the copolymer amphiphilic. Among the prepared SMA–POA amines with different POA–amines, the copolymers grafted with POP230 and POP400 are water-soluble, while the POP2000 grafting is insoluble. However, the consequent acidification with HCl to convert amine into amine salts may enhance the copolymer solubility in water or in water/ethanol (70/30 weight ratio). These copolymers are capable of emulsifying the toluene/water mixture and also lowering the toluene/water interfacial tension. In a preliminary screening experiment, it was found that the SMA3000 (prepared from 3:1 molar ratio of styrene to maleic anhydride) was more appropriate than SMA1000 or SMA6000 for preparing the amphiphilic copolymers. Their hydrophilic/hydrophobic balance is largely dependent on the structural variation with the SMA3000 as the suitable backbone for grafting with the POP amines. As shown in Figure 1, the SMA3000 polyamines with short POP pendent amines, such as POP230 and POP400, were enabled to reduce the interfacial tension effectively from 36 to 4 mN/m at a considerably low concentration (10^{-4} – 10^{-5} wt%) for the critical micelle concentration (cmc). By comparison, the grafting with 2000 M_w segmental weight pendants rendered the copolymer rather hydrophobic and soluble in toluene. The efficacy of the interfacial tension reduction was found to be less effective and required a higher concentration (10^{-1} – 10^{-2} wt%) to reach its cmc. With the grafting of hydrophilic poly(oxyethylene) seg-

Scheme 1. Synthesis of the Comb-Branched Copolymers from the POA–Diamine Grafting onto Poly(styrene-*co*-maleic anhydride)

ments (POE2000) of 2000 M_w , the resultant SMA3000–POE2000 was highly water-soluble. It demonstrated a better surfactancy than the POP2000 counterpart, but was less effective than SMA3000–POP400. The results imply that a proper balance of hydrophobic and hydrophilic functionalities in the structure is important for the amphiphilic copolymer. With the same SMA3000 backbone, the length of POP segmental weights of 230 and 400 g/mol is more appropriate for the amphiphilic property than the POP of 2000 g/mol. On the other hand, the acidification of SMA3000–POP400– H^+ had shifted the copolymer to be more hydrophilic but exhibited a slightly lower ability to reduce the toluene/water interfacial tension.

Intercalation and Ionic Exchange Reaction of the SMA Copolymers with Na^+ –MMT. The acidification to generate the corresponding cationic amines (SMA–POA amines– H^+) is required for ionic exchanging intercalation with Na^+ –MMT. During the intercalation, the counterions (Na^+) were replaced with the organic amine salts. With multiple ionic sites in the comb-branched structure, the exchange reaction with the sodium

ions may occur at multiple sites within the layered confinements. Structurally, the polyvalent pendent salts are highly effective for entering the clay gallery and tethering onto the surface of silicate platelets, while the SMA backbone is hydrophobic and may not intercalate into the clay interlayer. As a result, the POP–segments could be embedded in the silicate interlayer and the hydrophobic SMA remains in the surrounding corona phase. It is also possible that the SMA backbones be incorporated into the silicate gallery along with the polar POPs to yield an expanded d spacing. In fact, there were observed two classes of intercalated silicate hybrids of different d spacing depending on the POP lengths and SMA structures in the SMA–POP copolymers. As shown in Table 2, a low d spacing (12.9 and 14.8 Å) was observed for the POP230- and POP400-grafted SMA3000 (abbreviated as SMA3000–POP230– H^+ and SMA3000–POP400– H^+). With the lengthy POP pendants, the SMA3000–POP2000– H^+ and SMA3000–POP4000– H^+ copolymers afforded the silicate hybrids with a higher d spacing of 46.0 and 78.0 Å, respectively.

Previously, we have reported that the use of the pristine POP–diamines such as POP2000 and POP4000 could intercalate the Na^+ –MMT clay to reach 58.0 and 92.0 Å basal spacing, respectively.²⁰ The high spacing result was attributed to the hydrophobic POP2000 backbone aggregation in the gallery. The hydrophobic aggregation generated a new organic phase and enlarged the silicate d spacing. When using the POP–amine grafted SMA copolymers, such as SMA3000–POP2000 and SMA3000–POP4000, the d spacing was generally lower than that of the POP2000 and POP4000 diamines (Table 2). It appeared that the SMA backbone could restrict the POP incorporation or self-assembly in the gallery.

The presence of hydrophobic effect may be evidenced indirectly by comparing with the intercalation of the copolymer grafted with the hydrophilic POE2000 amine, which was expected to generate only low spacing such as 18.0 Å. The hydrophilic $-(CH_2CH_2O)_x-$ segment in the POE pendants favored a “flat” POE conformation in association with the surface of silicate platelets.²¹ However, the SMA backbone may

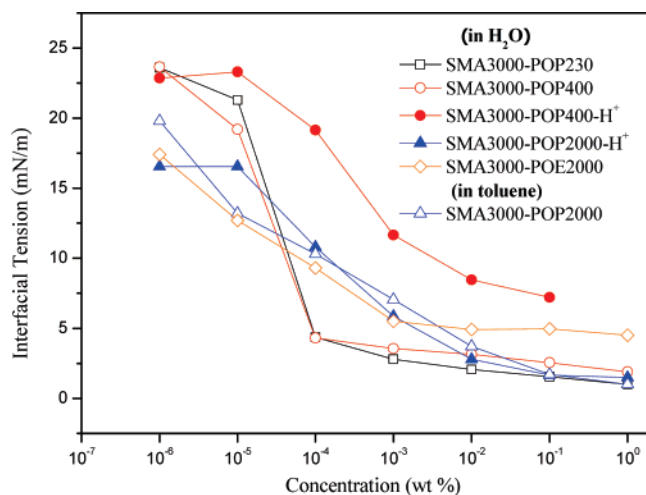


Figure 1. Amphiphilic property of the SMA–POP copolymers in reducing the toluene/water interfacial tension.

Table 2. Maximal Intercalation by the SMA–POP Comb-Branched Polyamines to Na⁺–MMT at Amine/CEC = 1.0/1.0 equiv Ratio

linear				comb-branched			
polyamines–H ⁺	<i>d</i> spacing (Å)	organics (wt %)		polyamines–H ⁺	<i>d</i> spacing (Å)	organics (wt %)	
		found by TGA ^a	calculated from CEC ^b			found by TGA ^a	calculated from CEC ^c
POP230	15.0	17	21	SMA3000–POP230	12.9	43	44
POP400	19.4	26	32	SMA3000–POP400	14.8	42	40
POP2000	58.0	63	70	SMA3000–POP2000	46.0	70	74
POP4000	92.0	75	82	SMA3000–POP4000	78.0	81	85
POE2000	19.0	43	70	SMA3000–POE2000	18.0	58	74
				SMA3000–POE2000 ^d	40.0	62	77

^a Organic wt % analyzed from TGA. ^b Calculated from CEC = 1.15 mequiv/g (clay from Kunimine Inc.) ^c Calculated from CEC = 1.40 mequiv/g (clay from Nanocor Inc.) ^d Amine/CEC = 1.2/1.0

Table 3. Solubility or Dispersion Ability of the SMA–POP Copolymers and the Copolymer/Silicate Hybrids

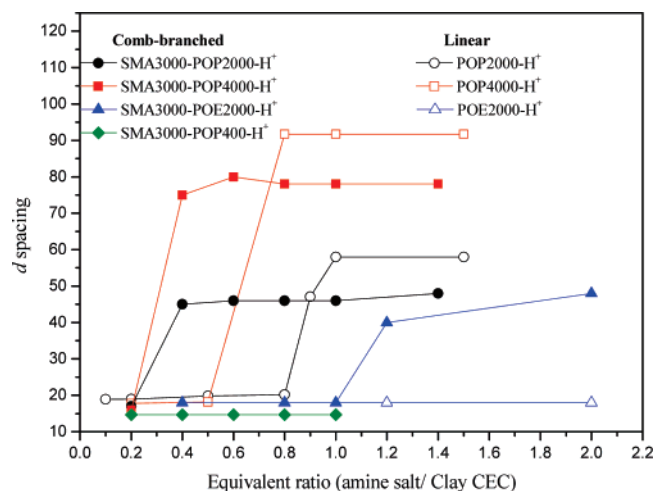
graft copolymers	H ₂ O	toluene	EtOH
SMA3000–POP230	+	–	+
SMA3000–POP400	+	–	+
SMA3000–POP2000	–	+	+
SMA3000–POP4000	–	+	+
SMA3000–POE2000	+	–	+
SMA3000–POP230–H ⁺	+	–	+
SMA3000–POP400–H ⁺	+	–	+
SMA3000–POP2000–H ⁺	+	+	+
SMA3000–POP4000–H ⁺	+	+	+
SMA3000–POE2000–H ⁺	+	–	+
SMA3000–POP230–H ⁺ /MMT	+-	–	+-
SMA3000–POP400–H ⁺ /MMT	+	–	+-
SMA3000–POP2000–H ⁺ /MMT	–	–	–
SMA3000–POP4000–H ⁺ /MMT	–	–	–
SMA3000–POE2000–H ⁺ /MMT	+-	–	+-

^a Key: (+) dispersible or soluble; (+–) dispersible but forming sediments after 2 h settlement; (–) not dispersible or insoluble.

join the interaction together with the POE embedment. In fact, the SMA3000–POE2000 copolymer could widen the gallery with 48 Å *d* spacing at amine/CEC = 1.2, a significant difference from the pristine POE2000 intercalation (18.0 Å). Judging from these results, the SMA backbone may also intercalate into the clay interlayer space in the case of wide spacing. Both POE2000- and POP2000-grafted SMA3000 could behave similarly in expanding the gallery when involved with the participation of the hydrophobic SMA backbone.

Dispersing Properties of SMA Copolymer Intercalated MMT. By varying the POP–amine pendent length, the polyamine intercalated hybrids may alter their dispersing properties from water-dispersible to toluene-dispersible. The solubility of these copolymers in water or organic solvents is actually dependent on the length of POPs, as shown in Table 3. Their solubility is generally increased when the amine copolymers are converted into amine salts after the HCl treatment. In the case of short POP230 and POP400 grafted SMA3000, the copolymers were water dispersible while the POP2000- and POP4000-analogs were toluene dispersible. By comparison, the copolymer grafted with the hydrophilic POE2000 was hydrophilic and dispersible only in water and the polar ethanol solvent.

Critical Conformational Change of the SMA–POP Copolymer Intercalating Na⁺–MMT. Two types of SMA–POP and SMA–POE comb-branched polyamines were allowed to intercalate into Na⁺–MMT under different amine–salt/CEC equivalent ratios. The intercalation profiles of SMA–POP polyamines were compared to those of POP2000, POP4000, and POE2000, as shown as Figure 2. By incrementally increasing the amine/CEC equiv ratio from 0.2 to 1.0, the intercalation of SMA3000–POP2000–H⁺ afforded hybrids with XRD *d* spacing increasing from 17 to 46 Å. It was found that the maximum silicate interlayer expansion space was reached at

**Figure 2.** Intercalation profiles of Na⁺–MMT with SMA–POP polyamines with respect to the CEC stoichiometry.

amine/CEC = 0.4. Beyond this equivalent ratio, the *d* spacing (46 Å) remained a constant regardless of the further increase of amine/CEC from 0.4 to 1.0. For comparison, there existed a critical intercalation point for the linear POP2000–H⁺ amine–salt at 0.8 equiv, reaching a higher *d* spacing of 58 Å. Similarly, the SMA3000–POP4000–H⁺ intercalation had a critical point at 0.4 equiv ratio and XRD spacing of 78 Å, in comparison with the sudden increase to 92 Å *d* spacing after the 0.5 CEC equiv for POP4000–H⁺. The nonlinear increasing of *d* spacing was caused by the hydrophobic aggregation in the confinement, a phenomenon similar to the critical micelle concentration (cmc) for surfactant molecules. The *d* spacing of the layered silicates was apparently affected by the hydrophobic aggregation of the hydrophobic POP and the SMA through the π – π interaction in the polystyrene portions. Because of the differences in the comb-branched structure and the hydrophobic character, it was observed that the SMA–POP pendent salts intercalated Na⁺–MMT with relatively low *d* spacing and also amine/CEC equiv for critical basal spacing.

Hydrophobic Effect of the SMA Backbone on Intercalation. The difference in the hydrophobic SMA backbones could influence the intercalation profile. The SMA–POP copolymers with different styrene/MA ratios in the backbone exhibited a range of gallery expansion. As demonstrated in Figure 3, the copolymer of 3:1 styrene/MA ratio such as in SMA3000–POP2000 may widen the *d* spacing up to 46 Å at 0.4 amine/CEC equiv, while the corresponding 1:1 styrene/MA backbone of SMA1000–POP2000 had an intercalation profile of 0.8 amine/CEC for the critical expansion and 25 Å basal spacing. These differences were attributed to the comb-branched structure of amine multiplicity and backbone hydrophobicity. With a very high polystyrene portion, the SMA6000–POP2000 and SMA11000–

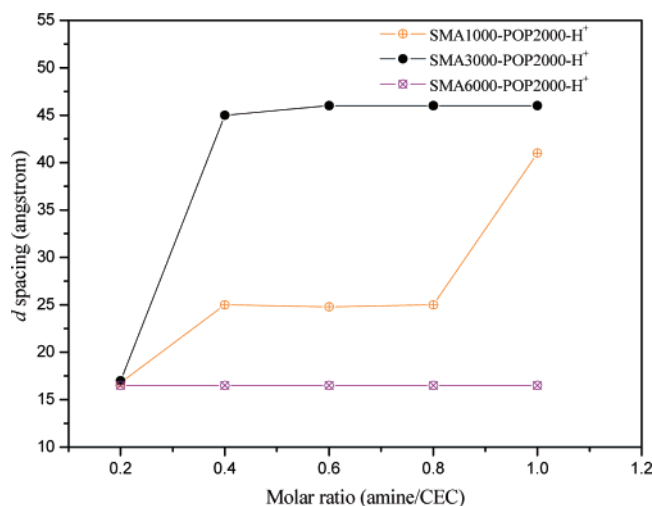


Figure 3. Intercalation profiles of Na^+ -MMT with the SMA-POP polyamines of different SMA backbones.

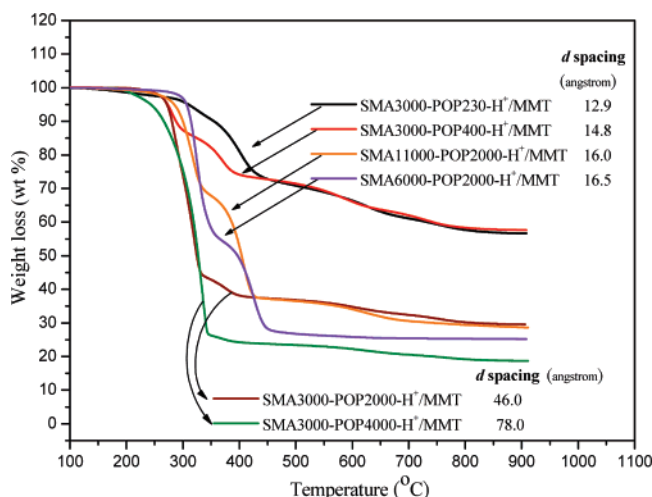


Figure 4. Thermal gravimetric analysis of the SMA-POP silicate hybrids.

POP2000 polyamines actually failed to intercalate Na^+ -MMT, perhaps due to the relatively low POP-amine affinity for clay or too high SMA hydrophobicity. The SMA3000 backbone was more suitable for the POP-amine grafting to generate the hydrophilic/hydrophobic balanced polyamines for the clay intercalation.

The intercalation of polyamines with different POP amine salts and hydrophobic SMA backbone had generated different hybrids possessing various organics involving the POP and SMA embedment. The short POP-amine grafted SMA such as SMA-POP230 and SMA-POP400 tended to intercalate into layered silicates with only low d spacing. On contrast, the lengthy POP amine-salts could expand the silicate gallery in a higher degree.

Differences in Thermal Degradation Patterns between the SMA-Crowned and SMA-Embedded Hybrids. The SMA-POP intercalated hybrids may exhibit different patterns of thermal stability under thermal gravimetric analysis. As summarized in Figure 4, both of the SMA3000-POP2000 and SMA3000-POP4000 hybrids with a large spacing (46 and 78 Å, respectively) demonstrated a sharp and single slope for the decomposition curve. In contrast, the hybrids of SMA3000-POP230 and SMA3000-POP400 hybrids were shown to be stepwise decomposed. The stepwise decomposition curves were also observed for the hybrids that were intercalated by the high

styrene/MA ratio backbone, such as SMA6000 and SMA11000. The hybrids of complicated TGA curves were often at a low d spacing of 12.9 ~ 16.5 Å. For example, the SMA11000-POP2000- H^+ /MMT was decomposed in two-step TGA pattern. In contrast, a sharp and single-step decomposition was observed for SMA3000-POP2000- H^+ /MMT with a d spacing of 48.0 Å. The different decomposition curves were attributed to whether the SMA organic fraction embedded in the layered silicates. Since the pristine SMA-POP itself exhibited only a simple decomposition curve, the silicate confinement was affecting the decomposition of the SMA backbone and POP portions. It is rationalized that the pendent POP-amine embedded in the silicates decomposed differently from that the SMA embedment. As a result, the hybrids were decomposed with more than one decomposing rate.

On the basis of TGA data, the organic fraction in the intercalated hybrids was measurable by calculating the amount of organic decomposition and the residues of inorganic silicates in TGA at high temperature. The weight ratio of organic to inorganic portions can be correlated to the hybrid d spacing which linearly increases with the organic embedding.²¹ In the series of the pristine POP-diamines of different molecular weights from POP230, POP400, POP2000, and POP4000, their intercalated silicates had the increasing d spacing from 15 to 92 Å corresponding to the increase of organic fraction (22–83 wt %). However, the d spacing of the polyamine-intercalated hybrids was deviated from the linear relationship with TGA organic composition.²² This was attributed to the hybrid structures that consisted of the SMA backbone that was surrounded the silicates without embedding into the silicate interlayer. The observations of different types of intercalated hybrids in d spacing and TGA organic analyses may be used to probe the intercalation mechanism. Depending on the hydrophobic nature of the SMA backbone and the ionic sites of the POP pendants, the intercalation modes may be different, one with only the POP embedment and another with POP/SMA together incorporated in the silicate gallery. As shown in Table 2, the hybrids intercalated with high SMA/POP fraction such as SMA3000-POP230 (12.9 Å; 43 wt %), SMA3000-POP400 (14.8 Å; 42 wt %), SMA6000-POP2000 (16.0 Å; 75 wt %), and SMA11000-POP2000 (16.5 Å; 71 wt %) exhibited a low d spacing, explained by low SMA intercalation. On the other hand, the hybrids with a high POP fraction such as SMA3000-POP2000 (46.0 Å; 70 wt %) and SMA3000-POP4000 (78.0 Å; 81 wt %) afforded a family of high basal spacing.

Crystallization Behaviors of the SMA-POE Copolymer Intercalated Silicate Hybrids. Since the poly(ethylene glycol)-based POE2000 diamine has a crystalline property, the thermal behavior of the grafted SMA-POE2000 may behave differently when embedded in the silicate confinement. In the SMA3000-POE2000 intercalation, the crystalline behaviors of POE2000 segments in the silicate gallery were characterized by using DSC analyses. The confinement effect was demonstrated by the different enthalpy of the POE crystallization, when the POE was embedded in the confinement with or without SMA participation. Shown in Figure 5 are the comparative results of the POE2000 starting amine, the SMA-POE2000 copolymer itself, and the intercalated organoclay. The melting point of the pristine POE2000 at $T_m = 34$ °C ($\Delta H = 123.1$ J/g) was compared to $T_m = 31$ °C ($\Delta H = 80.1$ J/g) for the SMA-POE2000 copolymer. A further restriction on the POE crystallization was observed for the SMA3000-POE2000- H^+ /MMT hybrid ($T_m = 21$ °C and $\Delta H = 0.2$ J/g). The restriction for the POE crystallization is known for the cases of POE2000,^{16a} poly-

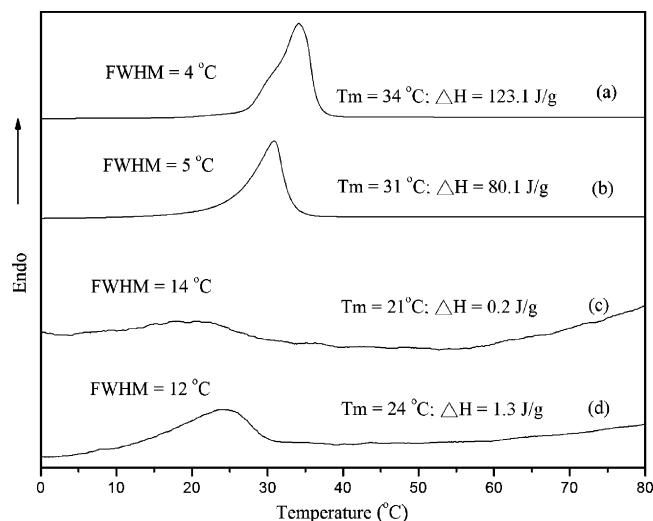


Figure 5. DSC analyses on crystallization behaviors of POE on the SMA side chains: (a) pristine POE2000 diamine; (b) SMA3000–POE2000; (c) SMA3000–POE2000–H⁺/MMT (intercalated at molar ratio 1.0, XRD = 18 Å); (d) SMA3000–POE2000–H⁺/MMT (intercalated at molar ratio 1.2, XRD = 40 Å).

(ethylene glycol),²² and SEBS-*g*-POE2000¹⁷ when embedded in the silicate gallery. However, the SMA–POE embedded silicates can be more complicated since the SMA backbone may participate with the POE embedment in the confinement. It was observed that the SMA–POE embedded silicates with a high 40 Å *d* spacing was less restricted ($T_m = 24$ °C and $\Delta H = 1.3$ J/g) for melting than that with 18.0 Å *d* spacing ($T_m = 21$ °C and $\Delta H = 0.4$ J/g). The width at half-maximum (fwhm) intensity of the crystallization peaks in DSC was used to compare the rate of induced crystallization in the confinement. The width (in degrees Celsius) of the crystallization peak implied the homogeneity of POE environment during the melting process. The hybrid of 40.0 Å *d* spacing showed a slightly narrower FWHM (12 °C) than that of 18 Å *d* spacing (14 °C), implying a fast rate of POE melting. Hence, different POE embedded hybrids were differentiated in the DSC analyses.

Conclusion

The use of the SMA–POA comb-branched polyamines, synthesized from the POA–amine grafting SMA, allowed us to systematically study the Na⁺–MMT intercalation. By varying the structures of SMA backbone and POA pendants, these polyamine salts may intercalate the silicate clay in different manners. With the structures of short POP on SMA3000 or lengthy POP on SMA6000, such as SMA3000–POP230, SMA3000–POP400, and SMA6000–POP2000, the copolymers intercalated MMT to afford the POP-embedded organoclays with a low *d* spacing. In contrast, the copolymers with the lengthy

POP amines, such as SMA1000–POP2000 and SMA3000–POP2000, may derive silicates with an embedment of both POP and SMA in the gallery and consequently a high expansion of *d* spacing. The driving force for this embedment arises from the ionic exchange reaction involving the multiple ionic sites in the copolymers with the sodium counterions in Na⁺–MMT. The intercalation was also influenced by the equivalent ratio of amine salts to the clay cation exchange capacity (CEC). The understanding of factors involving ionic exchanging and hydrophobic aggregation allows the preparation of new silicate hybrids for various applications.

Acknowledgment. We acknowledge the financial support from the National Science Council (NSC) of Taiwan.

References and Notes

- (1) Cseri, T.; Bekassy, S.; Figueras, F.; Rizner, S. *J. Mol. Catal. A* **1995**, 98, 101.
- (2) Celis, R.; Hermosin, M. C.; Carrizosa, M. J.; Cornejo, J. *J. Agric. Food Chem.* **2002**, 50, 2324.
- (3) Kiraly, Z.; Veisz, B.; Mastalir, A.; Kofarago, G. *Langmuir* **2001**, 17, 5381.
- (4) (a) Giannelis, E. P. *Adv. Mater.* **1996**, 35, 29. (b) Theng, B. K. G. *The Chemistry of Clay-Organic Reactions*, 2nd ed.; John Wiley & Sons: New York, 1974. (c) Olphen, H. V. *Clay Colloid Chemistry*, 2nd ed.; John Wiley & Sons: New York, 1997. (d) Alexandre, M.; Dubois, P. *Mater. Sci. Eng.* **2000**, 28, 1. (e) Ray, S. S.; Okamoto, M. *Prog. Polym. Sci.* **2003**, 28, 1539.
- (5) (a) Wang, Q.; Gao, Q.; Shi, J. *J. Am. Chem. Soc.* **2004**, 126, 14346. (b) Choy, J. H.; Kwak, S. Y.; Park, J. S.; Jeong, Y. J.; Portier, J. J. *Am. Chem. Soc.* **1999**, 121, 1399.
- (6) Yano, K.; Usuki, A.; Okada, A. *J. Polym. Sci., Part A: Polym. Chem.* **1997**, 35, 2289.
- (7) Wang, Z.; Pinnavaia, T. J. *Chem. Mater.* **1998**, 10, 1820.
- (8) Gilman, J. W. *Appl. Clay Sci.* **1999**, 15, 31.
- (9) Usuki, A.; Kojima, Y.; Kawasumi, M.; Okada, A.; Fukushima, Y.; Kurauchi, T.; Kamigaito, O. *J. Mater. Res.* **1993**, 8, 1179.
- (10) Bohning, M.; Goering, H.; Fritz, A.; Brzezinka, K. W.; Turkey, Scholnhals, G. A.; Scharrel, B. *Macromolecules* **2005**, 38, 2764.
- (11) Robello, D. R.; Yamaguchi, N.; Blanton, T.; Barnes, C. *J. Am. Chem. Soc.* **2004**, 126, 8118.
- (12) (a) Tien, Y. I.; Wei, K. H. *J. Appl. Polym. Sci.* **2002**, 86, 1741. (b) Kuan, H. C.; MA, C. C.; Chuang, W. P.; Su, H. Y. *J. Polym. Sci., Part B: Polym. Phys.* **2005**, 43, 1.
- (13) Lepoittevin, B.; Pantoustier, N.; Alexandre, M.; Calberg, C.; Jerome, R.; Dubois, P. *J. Mater. Chem.* **2002**, 12, 3528.
- (14) (a) Kong, D.; Park, C. E. *Chem. Mater.* **2003**, 15, 419. (b) Zelenkova, M.; Zelenka, J.; Spacek, V.; Socha, F. *Macromol. Symp.* **2003**, 200, 291.
- (15) (a) Fu, X.; Qutubuddin, S. *Mater. Lett.* **2000**, 42, 12. (b) Fu, X.; Qutubuddin, S. *Polymer* **2001**, 42, 807.
- (16) (a) Lin, J. J.; Cheng, I. J.; Wang, R.; Lee, R. J. *Macromolecules* **2001**, 34, 8832. (b) Chou, C. C.; Chang, Y. C.; Chiang, M. L.; Lin, J. J. *Macromolecules* **2004**, 37, 473.
- (17) Chang, Y. C.; Chou, C. C.; Lin, J. J. *Langmuir* **2005**, 21, 7023.
- (18) Chou, C. C.; Lin, J. J. *Macromolecules* **2005**, 38, 230.
- (19) Lin, J. J.; Hsu, Y. C.; Chou, C. C. *Langmuir* **2003**, 19, 5184.
- (20) Lin, J. J.; Chou, C. C. *Macromol. Rapid Commun.* **2003**, 24, 492.
- (21) Chou, C. C.; Shieu, F. S.; Lin, J. J. *Macromolecules* **2003**, 36, 2187.
- (22) Strawhecker, K. E.; Manias, E. *Chem. Mater.* **2000**, 12, 2943.

MA062508D